

Hands Deep in Deep Learning for Hand Pose Estimation

Markus Oberweger Paul Wohlhart Vincent Lepetit
Institute for Computer Graphics and Vision
Graz University of Technology, Austria
{oberweger, wohlhart, lepetit}@icg.tugraz.at

Abstract.

We introduce and evaluate several architectures for Convolutional Neural Networks to predict the 3D joint locations of a hand given a depth map. We first show that a prior on the 3D pose can be easily introduced and significantly improves the accuracy and reliability of the predictions. We also show how to use context efficiently to deal with ambiguities between fingers. These two contributions allow us to significantly outperform the state-of-the-art on several challenging benchmarks, both in terms of accuracy and computation times. The code can be found at <https://github.com/moberweger/deep-prior/>.

1. Introduction

Accurate hand pose estimation is an important requirement for many Human Computer Interaction or Augmented Reality tasks, and has attracted lots of attention in the Computer Vision research community [10, 11, 14, 15, 17, 22, 23, 29]. Even with 3D sensors such as structured-light or time-of-flight sensors, it is still very challenging, as the hand has many degrees of freedom, and exhibits self-similarity and self-occlusions in images.

Given the current trend in Computer Vision, it is natural to apply Deep Learning [18] to solve this task, and a Convolutional Neural Network (CNN) with a standard architecture performs remarkably well when applied to this problem, as a simple experiment shows. However, the layout of the network has a strong influence on the accuracy of the output [4, 21] and in this paper, we aim at identifying the architecture that performs best for this problem.

More specifically, our contribution is two-fold:

- We show that we can learn a prior model of the hand pose and integrate it seamlessly to the network to improve the accuracy of the predicted

pose. This results in a network with an unusual “bottleneck”, *i.e.* a layer with fewer neurons than the last layer.

- Like previous work [21, 27], we use a refinement stage to improve the location estimates for each joint independently. Since it is a regression problem, spatial pooling and subsampling should be used carefully for this stage. To solve this problem, we use multiple input regions centered on the initial estimates of the joints, with very small pooling regions for the smaller input regions, and larger pooling regions for the larger input regions. Smaller regions provide accuracy, larger regions provide contextual information.

We show that our original contributions allow us to significantly outperform the state-of-the-art on several challenging benchmarks [22, 26], both in terms of accuracy and computation times. Our method runs at over 5000 fps on a single GPU and over 500 fps on a CPU, which is one order of magnitude faster than the state-of-the-art.

In the remainder of the paper, we first give a short review of related work in Section 2. We introduce our contributions in Section 3 and evaluate them in Section 4.

2. Related Work

Hand pose estimation is an old problem in Computer Vision, with early references from the nineties, but it is currently very active probably because of the appearance of depth sensors. A good overview of earlier work is given in [6]. Here we will discuss only more recent work, which can be divided into two main approaches.

The first approach is based on generative, model-based tracking methods. [15, 17] use a 3D hand

model and Particle Swarm Optimization to handle the large number of parameters to estimate. [14] also considers dynamics simulation of the 3D model. Several works rely on a tracking-by-synthesis approach: [5] considers shading and texture, [1] salient points, and [29] depth images. All these works require careful initialization in order to guarantee convergence and therefore rely on tracking based on the last frames’ pose or separate initialization methods—for example, [17] requires the fingertips to be visible. Such tracking-based methods have difficulty handling drastic changes between two frames, which are common as the hand tends to move fast.

The second type of approach is discriminative, and aims at directly predicting the locations of the joints from RGB or RGB-D images. For example, [11] and [13] rely on multi-layered Random Forests for the prediction. The former uses invariant depth features, and the latter uses clustering in hand configuration space and pixel-wise labelling. However, both do not predict the actual 3D pose but only classify given poses based on a dictionary. Motivated by work for human pose estimation [20], [10] uses Random Forests to perform a per-pixel classification of depth images and then a local mode-finding algorithm to estimate the 2D joint locations. However, this approach cannot directly infer the locations of hidden joints, which are much more frequent for hands than for the human body.

[23] proposed a semi-supervised regression forest, which first classifies the hands viewpoint, then the individual joints, to finally predict the 3D joint locations. However, it relies on a costly pixel-wise classification, and requires a huge training database due to viewpoint quantization. The same authors proposed a regression forest in [22] to directly regress the 3D locations of the joints, using a hierarchical model of the hand. However, their hierarchical approach accumulates errors, causing larger errors for the finger tips.

Even more recently, [26] uses a CNN for feature extraction and generates small “heatmaps” for joint locations from which they infer the hand pose using inverse kinematics. However, their approach predicts only the 2D locations of the joints, and uses a depth map for the third coordinate, which is problematic for hidden joints. Furthermore, the accuracy is restricted to the heatmap resolution, and creating heatmaps is computationally costly as the CNN has to be evaluated at each pixel location.

The hand pose estimation problem is of course closely related to the human body pose estimation problem. To tackle this problem, [20] proposed per-pixel semantic segmentation and regression forests to estimate the 3D human body pose from a single depth image. [9] recently showed it was possible to do the same from RGB images only, by combined body part labelling and iterative structured-output regression for 3D joint localization. [27] recently proposed a cascade of CNNs to directly predict and iteratively refine the 2D joint locations in RGB images. Further, [25] used a CNN for part detection and a simple spatial model, which however, is not effective for high variations in pose space.

In our work, we build on the success of CNNs and use them for their demonstrated performance. We observe, that the structure of the network is very important. Thus we propose and investigate different architectures to find the most appropriate one for the hand pose estimation problem. We propose a network structure that works very well, outperforming the baselines on two difficult datasets.

3. Hand Pose Estimation with Deep Learning

In this section we present our original contributions to the hand pose estimation problem. We first briefly introduce the problem and a simple 2D hand detector, which we use to get a coarse bounding box of the hand as input to the CNN-based pose predictors.

Then we describe our general approach which consists of two stages. For the first stage we consider different architectures that predict the locations of all joints simultaneously. Optionally, this stage can predict the pose in a lower-dimensional space, which is described next. Finally, we detail the second stage, which refines the locations of the joints independently from the predictions made at the first stage.

3.1. Problem Formulation

We want to estimate the J 3D hand joint locations $\mathbf{J} = \{\mathbf{j}_i\}_{i=1}^J$ with $\mathbf{j}_i = (x_i, y_i, z_i)$ from a single depth image. We assume that a training set of depth images labeled with the 3D joint locations is available. To simplify the regression task, we first estimate a coarse 3D bounding box containing the hand using a simple method similar to [22], by assuming the hand is the closest object to the camera: We extract from the depth map a fixed-size cube centered on the cen-

ter of mass of this object, and resize it to a 128×128 patch of depth values normalized to $[-1, 1]$. Points for which the depth is not available—which may happen with structured light sensors for example—or are deeper than the back face of the cube, are assigned a depth of 1. This normalization is important for the CNN in order to be invariant to different distances from the hand to the camera.

3.2. Network Structures for Predicting the Joints’ 3D Locations

We first considered two standard CNN architectures. The first one is shown in Fig. 1a, and is a simple shallow network, which consists of a single convolutional layer, a max-pooling layer, and a single fully-connected hidden layer. The second architecture we consider is shown in Fig. 1b and is a deeper but still generic network [12, 27], with three convolutional layers followed by max-pooling layers and two fully-connected hidden layers. All layers use Rectified Linear Unit [12] activation functions.

Additionally, we evaluated a multi-scale approach, as done for example in [7, 19, 25]. The motivation for this approach is that using multiple scales may help capturing contextual information. It uses several downscaled versions of the input image as input to the network, as shown in Fig. 1c.

Our results will show that, unsurprisingly, the multi-scale approach performs better than the deep architecture, which performs better than the shallow one. However, our contributions, described in the next two sections, bring significantly more improvement.

3.3. Enforcing a Prior on the 3D Pose

So far we only considered predicting the 3D positions of the joints directly. However, given the physical constraints over the hand, there are strong correlation between the different 3D joint locations, and previous work [28] has shown that a low dimensional embedding is sufficient to parameterize the hand’s 3D pose. Instead of directly predicting the 3D joint locations, we can therefore predict the parameters of the pose in a lower dimensional space. As this enforces constraints of the hand pose, it can be expected that it improves the reliability of the predictions, which will be confirmed by our experiments.

As shown in Fig. 1d, we implement the pose prior into the network structure by introducing a “bottleneck” in the last layer. This bottleneck is a layer with

less neurons than necessary for the full pose representation, *i.e.* $\ll 3 \cdot J$. It forces the network to learn a low dimensional representation of the training data, that implements the physical constraints of the hand. Similar to [28], we rely on a linear embedding. The embedding is enforced by the bottleneck layer and the reconstruction from the embedding to pose space is integrated as a separate hidden layer added on top of the bottleneck layer. The weights of the reconstruction layer are set to compute the back-projection into the $3 \cdot J$ -dimensional joint space. The resulting network therefore directly computes the full pose. We initialize the reconstruction weights with the major components from a Principal Component Analysis of the hand pose data and then train the full network using back-propagation. Using this approach we train the networks described in the previous section.

The embedding can be as small as 8 dimensions for a 42-dimensional pose vector to fully represent the 3D pose as we show in the experiments.

3.4. Refining the Joint Location Estimates

The previous architectures provide estimates for the locations of all the joints simultaneously. As done in [21, 27], these estimates can then be refined independently.

Spatial context is important for this refinement step to avoid confusion between the different fingers. The best performing architecture we experimented with is shown in Fig. 2a. We will refer to this architecture as *ORRef*, for Refinement with Overlapping Regions. It uses as input several patches of different sizes but all centered on the joint location predicted by the first stage. No pooling is applied to the smallest patch, and the size of the pooling regions then increases with the size of the patch. The larger patches provide more spatial context, whereas the absence of pooling on the small patch enables better accuracy.

We also considered a standard CNN architecture as a baseline, represented in Fig. 1b, which relies on a single input patch. We will refer to this baseline as *StdRef*, for Refinement with Standard Architecture.

To further improve the accuracy of the location estimates, we iterate this refinement step several times, by centering the network on the location predicted at the previous iteration.

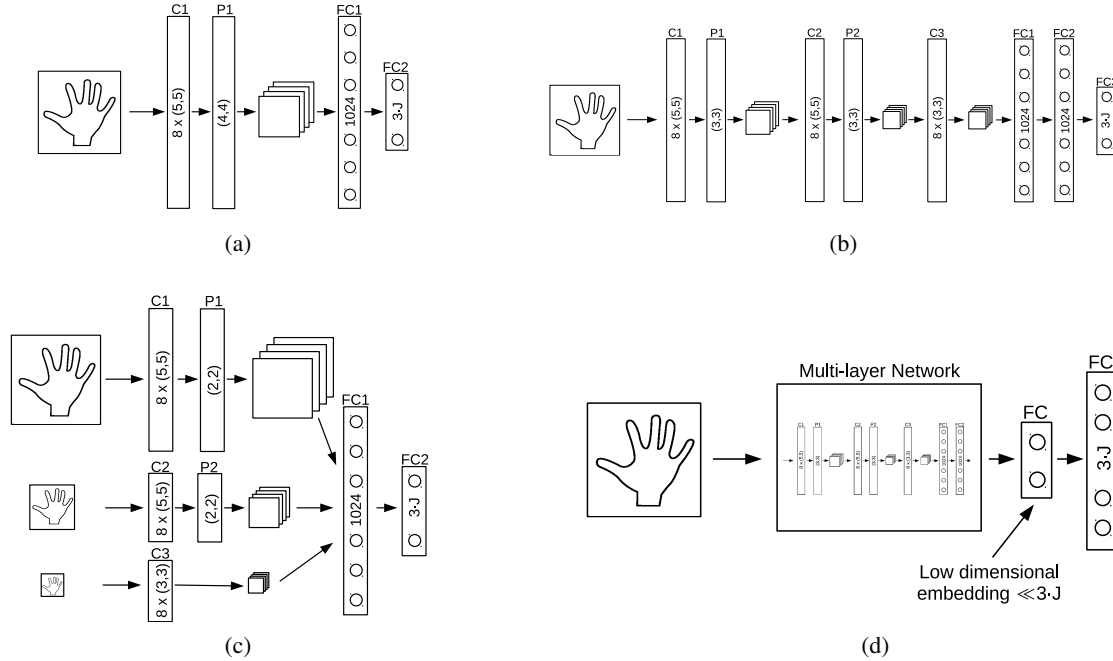


Figure 1: Different network architectures for the first stage. **C** denotes a convolutional layer with the number of filters and the filter size inscribed, **FC** a fully connected layer with the number of neurons, and **P** a max-pooling layer with the pooling size. We evaluated the performance of a shallow network (a) and a deeper network (b), as well as a multi-scale architecture (c), which was used in [7, 19]. This architecture extracts features after downscaling the input depth map by several factors. (d) All these networks can be extended to incorporate the constrained pose prior. This causes an unusual bottleneck with less neurons than the output layer.

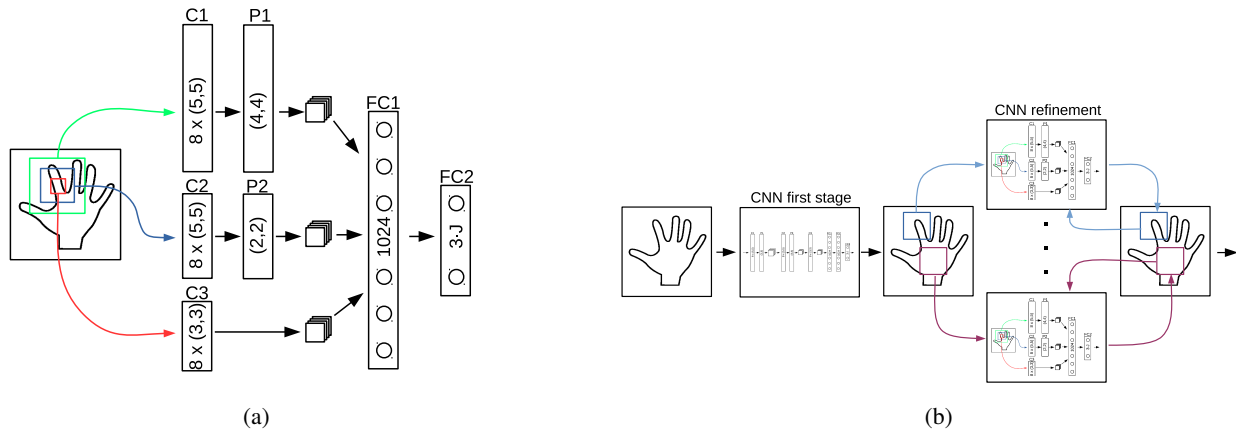


Figure 2: Our architecture for refining the joint locations during the second stage. We use a different network for each joint, to refine its location estimate as provided by the first stage. (a) The architecture we propose uses overlapping inputs centered on the joint to refine. Pooling with small regions is applied to the smaller inputs, while the larger inputs are pooled with larger regions. The smaller inputs allow for higher accuracy, the larger ones provide contextual information. We experimentally show that this architecture is more accurate than a more standard network architecture. (b) shows a generic architecture of an iterative refinement, where the output of the previous iteration is used as input for the next. As for Fig. 1, **C** denotes a convolutional layer, **FC** a fully connected layer, and **P** a max-pooling layer. (Best viewed in color)

4. Evaluation

In this section we evaluate the different architectures introduced in the previous section on several challenging benchmarks. We first introduce these benchmarks and the parameters of our meth-

ods. Then we describe the evaluation metric, and finally we present the results, quantitatively as well as qualitatively. Our results show that our different contributions significantly outperform the state-of-the-art.

4.1. Benchmarks

We evaluated our methods on the two following datasets:

NYU Hand Pose Dataset [26]: This dataset contains over 72k training and 8k test frames of RGB-D data captured using the Primesense Carmine 1.09. It is a structured light-based sensor and the depth maps have missing values mostly along the occluding boundaries as well as noisy outlines. For our experiments we use only the depth data. The dataset has accurate annotations and exhibits a high variability of different poses. The training set contains samples from a single user and the test set samples from two different users. The ground truth annotations contain $J = 36$ joints, however [26] uses only $J = 14$ joints, and we did the same for comparison purposes.

ICVL Hand Posture Dataset [22]: This dataset comprises a training set of over 180k depth images showing various hand poses. The test set contains two sequences with each approximately 700 depth maps. The dataset is recorded using a time-of-flight Intel Creative Interactive Gesture Camera and has $J = 16$ annotated joints. Although the authors provide different artificially rotated training samples, we only use the genuine 22k. The depth images have a high quality with hardly any missing depth values, and sharp outlines with little noise. However, the pose variability is limited compared to the NYU dataset. Also, a relatively large number of samples both from the training and test sets are incorrectly annotated: We evaluated the accuracy and about 36% of the poses from the test set have an annotation error of at least 10 mm.

4.2. Meta-Parameters and Optimization

The performance of neural networks depends on several meta-parameters, and we performed a large number of experiments varying the meta-parameters for the different architectures we evaluated. We report here only the results of the best performing sets of meta-parameters for each method. However, in our experiments, the performance depends more on the architecture itself than on the values of the meta-parameters.

We trained the different architectures by minimizing the distance between the prediction and the expected output per joint, and a regularization term for

weight decay to prevent over-fitting, where the regularization factor is 0.001. We do not differ between occluded and non-occluded joints. Because the annotations are noisy, we use the robust Huber loss [8] to evaluate the differences. The networks are trained with back-propagation using Stochastic Gradient Descent [3] with a batch size of 128 for 100 epochs. The learning rate is set to 0.01 and we use a momentum of 0.9 [16].

4.3. Evaluation Metrics

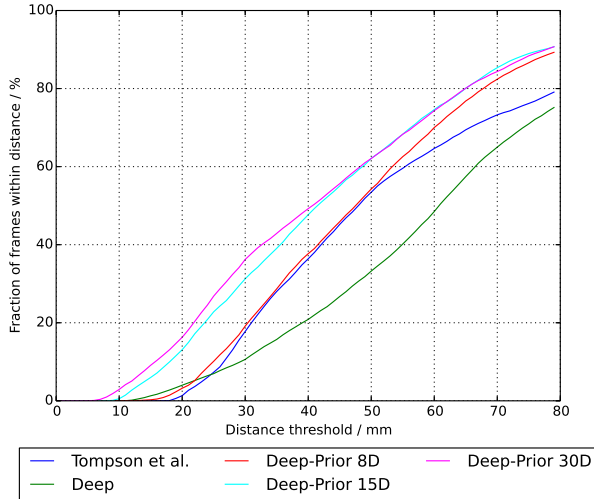
We use two different evaluation metrics:

- the average Euclidean distance between the predicted 3D joint location and the ground truth, and
- the fraction of test samples that have all predicted joints below a given maximum Euclidean distance from the ground truth, as was done in [24]. This metric is generally regarded very challenging, as a single dislocated joint deteriorates the whole hand pose.

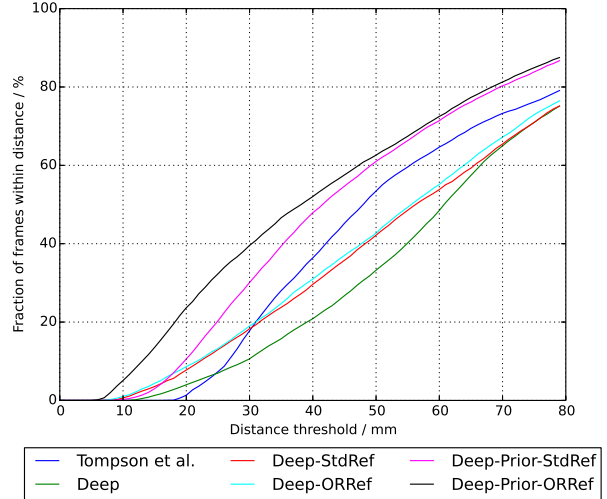
4.4. Importance of the Pose Prior

In Fig. 3a and 3c we compare different embedding dimensions and direct regression in the full $3 \cdot J$ -dimensional pose space for the NYU and the ICVL dataset, respectively. The evaluation on both datasets shows that enforcing a pose prior is beneficial compared to direct regression in the full pose space. Only 8 dimensions out of the original 42- or 48-dimensional pose spaces are already enough to capture the pose and outperform the baseline on both datasets. However, the 30-dimensional embedding performs best, and thus we use this for all further evaluations. The results on the ICVL dataset, which has noisy annotations, are not as drastic, but still consistent with the results on the NYU dataset.

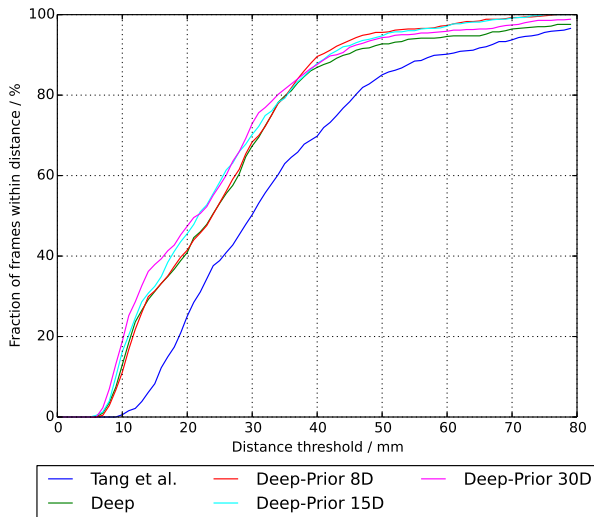
The baseline on the NYU dataset of Tompson *et al.* [26] only provide the 2D locations of the joints. For comparison, we follow their protocol and augment their 2D locations by taking the depth of each joint directly from the depth maps to derive comparable 3D locations. Depth values that do not lie within the hand cube are truncated to the cube's back face to avoid large errors. This protocol, however, has a certain influence on the error metric, as evident in Fig. 4a. The augmentation works well for some joints, as apparent by the average error. However, it is unlikely that the augmented depth is correct for



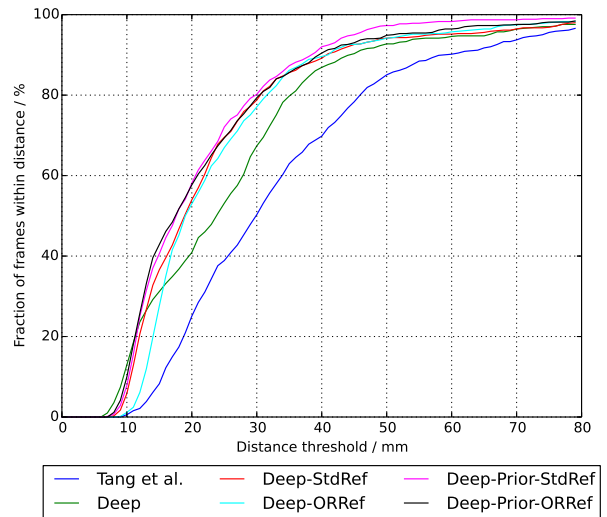
(a) Pose Prior on NYU dataset



(b) Refinement on NYU dataset



(c) Pose Prior on ICVL dataset



(d) Refinement on ICVL dataset

Figure 3: Importance of the pose prior (left) and the refinement stage (right). We evaluate the fraction of frames where all joints are within a maximum distance for different approaches. A higher area under the curve denotes more accurate results. **Left (a), (c):** We show the influence of the dimensionality of the pose embedding. The optimal value is around 30, but using only 8 dimensions performs already very well. The pose prior allows us to significantly outperform the state-of-the-art, even before the refinement step. **Right (b), (d):** We show that our architecture with overlapping input patches, denoted by the *ORRef* suffix, provides higher accuracy for refining the joint positions compared to a standard deep CNN, denoted by the *StdRef* suffix. For the baseline of Tompson *et al.* [26] we augment their 2D joint locations with the depth from the depth maps, as done by [26], and depth values that do not lie within the hand cube are truncated to the cube’s back face to avoid large errors. (Best viewed on screen)

all joints of the hand, *e.g.* the 2D joint location lies on the background or is self-occluded, thus causing higher errors for individual joints. When using the evaluation metric of [24], where all joints have to be within a maximum distance, this outlier has a strong influence, in contrast to the evaluation of the average error, where an outlier can be insignificant for the mean. Thus we outperform the baseline more signif-

icantly for the distance threshold than for the average error.

4.5. Increasing Accuracy with Pose Refinement

The refinement stage can be used to further increase the location accuracy of the predicted joints. We achieved the highest accuracy by using our CNN with constrained prior hand model as first stage, and

then applying the second iterative refinement stage with our CNN with overlapping input patches, denoted *ORRef*.

The results in Fig. 3b, 3d and 4 show that applying the refinement improves the location accuracy for different base CNNs. From rather inaccurate initial estimates, as provided by the standard deep CNN, our proposed ORRef performs only slightly better than refinement with the baseline deep CNN, denoted by *StdRef*. This is because for large initial errors only the larger input patch provides enough context for reasoning about the offset. The smaller input patch cannot provide any information if the offset is bigger than the patch size. For more accurate initial estimates, as provided by our deep CNN with pose prior, the ORRef takes advantage from the small input patch which does not use pooling for higher accuracy. We iterate our refinement two times, since iterating more often does not provide any further increase in accuracy.

We would like to emphasize that our results on the ICVL dataset, with an average accuracy below 10 mm, already scratch at the uncertainty of the labelled annotations. As already mentioned, the ICVL dataset suffers from inaccurate annotations, as we show in some qualitative samples in Fig. 5 first and fourth column. While this has only a minor effect on training, the evaluation is more affected. We evaluated the accuracy of the test sequence by revising the annotations in image space and calculated an average error of 2.4 mm with a standard deviation of 5.2 mm.

4.6. Running Times

Table 1 provides a comparison of the running times of the different methods, both on CPU and GPU. They were measured on a computer equipped with an Intel Core i7, 16GB of RAM, and an nVidia GeForce GTX 780 Ti GPU. Our methods are implemented in Python using the Theano library [2], which offers an option to select between the CPU and the GPU for evaluating CNNs. Our different models perform very fast, up to over 5000 fps on a single GPU. Training takes about five hours for each CNN. The deep network with pose prior performs very fast and outperforms all other methods in terms of accuracy. However, we can further refine the joint locations at the cost of higher runtime.

4.7. Qualitative Results

We present qualitative results in Fig. 5. The typical problems of structured light-based sensors, such

Architecture	GPU	CPU
Shallow	0.07 ms	1.85 ms
Deep [12]	0.1 ms	2.08 ms
Multi-Scale [7]	0.81 ms	5.36 ms
Deep-Prior	0.09 ms	2.29 ms
Refinement	2.38 ms	62.91 ms
Tompson <i>et al.</i> [26]	5.6 ms	-
Tang <i>et al.</i> [22]	-	16 ms

Table 1: Comparison of different runtimes. Our CNN with pose prior (*Deep-Prior*) is faster by a magnitude compared to the other methods (pose estimation only). We can further increase the accuracy using the refinement stage, still at competitive speed. All of the denoted baselines use state-of-the-art hardware comparable to ours.

as missing depth, can be problematic for accurate localization. However, only partially missing parts, as shown in the third and fourth columns for example, do not significantly deteriorate the result. The location of the joint is constrained by the learned hand model. If the missing regions get too large, as shown in the fifth column, the accuracy gets worse. However, because of the use of the pose subspace embedding, the predicted joint locations still preserve the learned hand topology. The erroneous annotations of the ICVL dataset deteriorate the results, as our predicted locations during the first stage are sometimes more accurate than the ones obtained during the second stage: see for example the pinky in the first or fourth column.

5. Conclusion

We evaluated different network architectures for hand pose estimation by directly regressing the 3D joint locations. We introduced a constrained prior hand model that can significantly improve the joint localization accuracy. Further, we applied a joint-specific refinement stage to increase the localization accuracy. We have shown, that for this refinement a CNN with overlapping input patches with different pooling sizes can benefit from both, input resolution and context. We have compared the architectures on two datasets and shown that they outperform previous state-of-the-art both in terms of localization accuracy and speed.

Acknowledgements: This work was funded by the Christian Doppler Laboratory for Handheld Augmented Reality and the TU Graz FutureLabs fund.

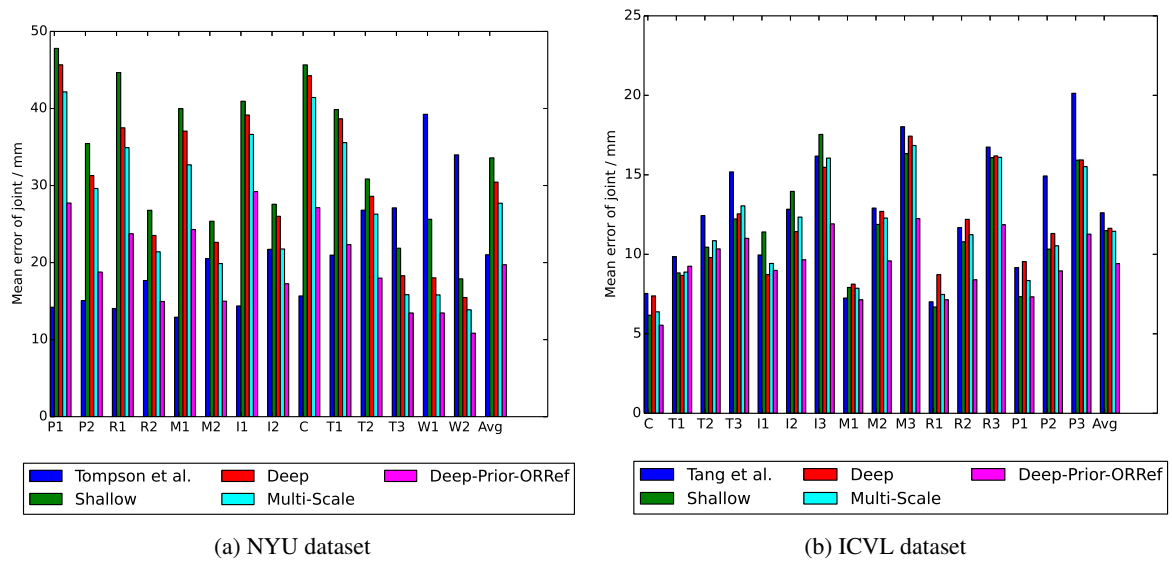


Figure 4: Average joint errors. For completeness and comparability we show the average joint errors, which are, however, not as decisive as the evaluation in Fig. 3. Though, the results are consistent. The evaluation of the average error is more tolerant to larger errors of a single joint, which deteriorate the pose as for Fig. 3, but are insignificant for the mean if the other joints are accurate. Our proposed architecture *Deep-Prior-ORRef*, the constrained pose CNN with refinement stage, provides the highest accuracy. For the ICVL dataset, the simple baseline architectures already outperform the baseline. However, they cannot capture the higher variations in pose space and noisy images of the NYU dataset, where they perform much worse. The palm and fingers are indexed as C: palm, T: thumb, I: index, M: middle, R: ring, P: pinky, W: wrist. (Best viewed on screen)

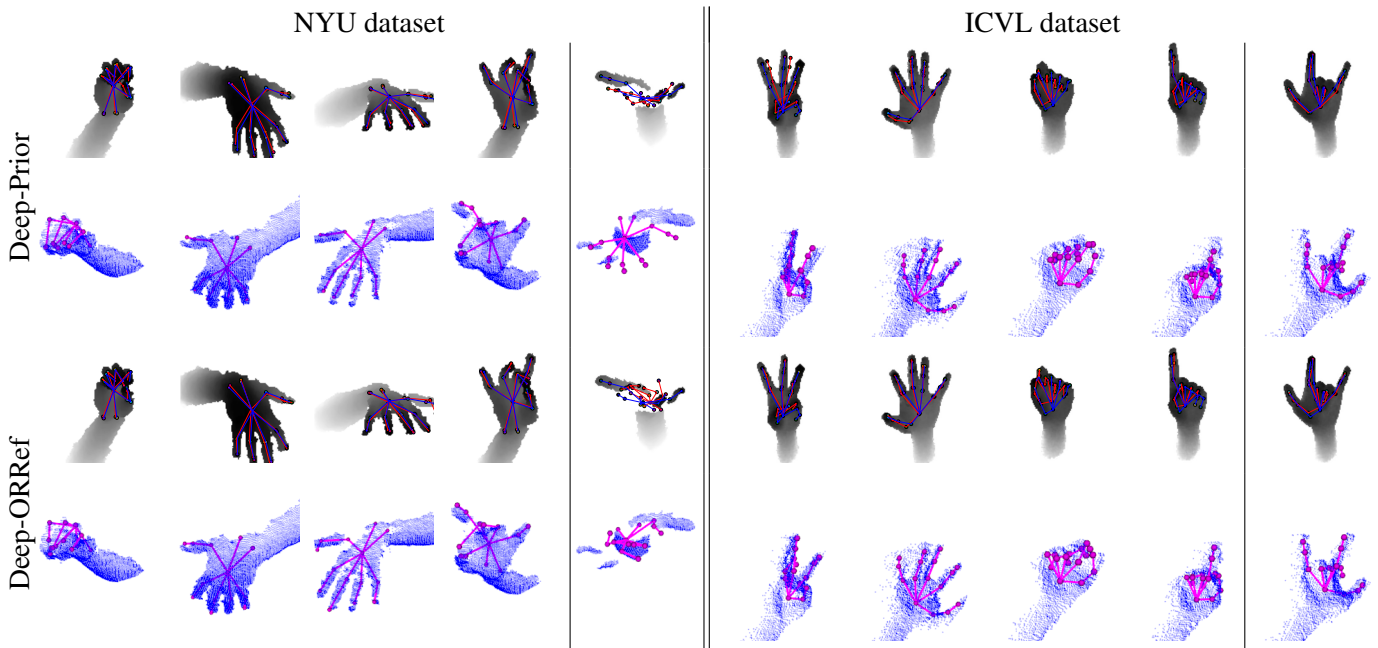


Figure 5: Qualitative results. We show the inferred joint locations on the depth images (in gray-scale), as well as the 3D locations with the point cloud of the hand (blue images) from a different angle. The ground truth is shown in blue, our results in red. The point cloud is only annotated with our results for clarity. The right columns show some erroneous results. One can see the difference between the global constrained pose and the local refinement, especially in the presence of missing depth values as shown in the fifth column. While the global pose constraint still preserves the hand topology, the local refinement cannot reason about the locations without the missing depth data. (Best viewed on screen)

References

- [1] L. Ballan, A. Taneja, J. Gall, L. V. Gool, and M. Pollefeys. Motion Capture of Hands in Action Using Discriminative Salient Points. In *European Conference on Computer Vision*, 2012.
- [2] J. Bergstra, O. Breuleux, F. Bastien, P. Lamblin, R. Pascanu, G. Desjardins, J. Turian, D. Warde-Farley, and Y. Bengio. Theano: A CPU and GPU Math Expression Compiler. In *Proc. of SciPy*, 2010.
- [3] L. Bottou. Large-Scale Machine Learning with Stochastic Gradient Descent. In *Proc. of COMPSTAT*, 2010.
- [4] A. Coates, A. Y. Ng, and H. Lee. An Analysis of Single-Layer Networks in Unsupervised Feature Learning. In *Proc. of AISTATS*, 2011.
- [5] M. de La Gorce, D. J. Fleet, and N. Paragios. Model-Based 3D Hand Pose Estimation from Monocular Video. *IEEE Transactions on Pattern Analysis and Machine Intelligence*, 33(9), 2011.
- [6] A. Erol, G. Bebis, M. Nicolescu, R. D. Boyle, and X. Twombly. Vision-Based Hand Pose Estimation: A Review. *Computer Vision and Image Understanding*, 108(1-2), 2007.
- [7] C. Farabet, C. Couprie, L. Najman, and Y. LeCun. Learning Hierarchical Features for Scene Labeling. *IEEE Transactions on Pattern Analysis and Machine Intelligence*, 2013.
- [8] P. J. Huber. Robust Estimation of a Location Parameter. *Annals of Statistics*, 53, 1964.
- [9] C. Ionescu, J. Carreira, and C. Sminchisescu. Iterated Second-Order Label Sensitive Pooling for 3D Human Pose Estimation. In *Conference on Computer Vision and Pattern Recognition*, 2014.
- [10] C. Keskin, F. Kır aç, Y. E. Kara, and L. Akarun. Real Time Hand Pose Estimation Using Depth Sensors. In *International Conference on Computer Vision*, 2011.
- [11] C. Keskin, F. Kır aç, Y. E. Kara, and L. Akarun. Hand Pose Estimation and Hand Shape Classification Using Multi-Layered Randomized Decision Forests. In *European Conference on Computer Vision*, 2012.
- [12] A. Krizhevsky, I. Sutskever, and G. E. Hinton. Imagenet Classification with Deep Convolutional Neural Networks. In *Advances in Neural Information Processing Systems*, 2012.
- [13] A. Kuznetsova, L. Leal-taix e, and B. Rosenhahn. Real-Time Sign Language Recognition Using a Consumer Depth Camera. In *International Conference on Computer Vision*, 2013.
- [14] S. Melax, L. Keselman, and S. Orsten. Dynamics Based 3D Skeletal Hand Tracking. In *Proc. of Graphics Interface Conference*, 2013.
- [15] I. Oikonomidis, N. Kyriazis, and A. A. Argyros. Full DOF Tracking of a Hand Interacting with an Object by Modeling Occlusions and Physical Constraints. In *International Conference on Computer Vision*, 2011.
- [16] B. T. Polyak. Some Methods of Speeding Up the Convergence of Iteration Methods. *USSR Computational Mathematics and Mathematical Physics*, 4(5), 1964.
- [17] C. Qian, X. Sun, Y. Wei, X. Tang, and J. Sun. Realtime and Robust Hand Tracking from Depth. In *Conference on Computer Vision and Pattern Recognition*, 2014.
- [18] J. Schmidhuber. Deep Learning in Neural Networks: An Overview. Technical Report 03-14, IDSIA, 2014.
- [19] P. Sermanet, D. Eigen, X. Zhang, M. Mathieu, R. Fergus, and Y. LeCun. Overfeat: Integrated Recognition, Localization and Detection Using Convolutional Networks. In *Proc. of ICRL*, 2014.
- [20] J. Shotton, R. Girshick, A. Fitzgibbon, T. Sharp, M. Cook, M. Finocchio, R. Moore, P. Kohli, A. Criminisi, A. Kipman, and A. Blake. Efficient Human Pose Estimation from Single Depth Images. In *Conference on Computer Vision and Pattern Recognition*, 2011.
- [21] Y. Sun, X. Wang, and X. Tang. Deep Convolutional Network Cascade for Facial Point Detection. In *Conference on Computer Vision and Pattern Recognition*, 2013.
- [22] D. Tang, H. J. Chang, A. Tejani, and T.-K. Kim. Latent Regression Forest: Structured Estimation of 3D Articulated Hand Posture. In *Conference on Computer Vision and Pattern Recognition*, 2014.
- [23] D. Tang, T. Yu, and T. Kim. Real-Time Articulated Hand Pose Estimation Using Semi-Supervised Transductive Regression Forests. In *International Conference on Computer Vision*, 2013.
- [24] J. Taylor, J. Shotton, T. Sharp, and A. Fitzgibbon. The Vitruvian Manifold: Inferring Dense Correspondences for One-Shot Human Pose Estimation. In *Conference on Computer Vision and Pattern Recognition*, 2012.
- [25] J. Tompson, A. Jain, Y. LeCun, and C. Bregler. Joint Training of a Convolutional Network and a Graphical Model for Human Pose Estimation. In *Advances in Neural Information Processing Systems*, 2014.
- [26] J. Tompson, M. Stein, Y. LeCun, and K. Perlin. Real-Time Continuous Pose Recovery of Human Hands Using Convolutional Networks. *ACM Transactions on Graphics*, 33, 2014.
- [27] A. Toshev and C. Szegedy. DeepPose: Human Pose Estimation via Deep Neural Networks. In *Conference on Computer Vision and Pattern Recognition*, 2014.
- [28] Y. Wu, J. Lin, and T. Huang. Capturing Natural Hand Articulation. In *International Conference on Computer Vision*, 2001.

- [29] C. Xu and L. Cheng. Efficient Hand Pose Estimation from a Single Depth Image. In *International Conference on Computer Vision*, 2013.